

Finite Element Analysis of the Multiple Drilling Technique for Early Osteonecrosis of the Femoral Head

JI YONG BAE,¹ DAI SOON KWAK,² KYUNG SOON PARK,³ and INSU JEON¹

¹School of Mechanical Systems Engineering, Chonnam National University, 300 Yongbong-dong, Buk-gu, Gwangju 500-757, Republic of Korea; ²Department of Anatomy, Catholic Institute for Applied Anatomy, College of Medicine, The Catholic University of Korea, 505 Banpo-dong, Seocho-gu, Seoul 137-040, Republic of Korea; and ³The Center for Joint Disease, Hwasun Hospital, Chonnam National University, 160 Ilsimri, Hwasun-Eup, Hwasun-Gun 519-809, Jeonnam, Republic of Korea

(Received 19 December 2012; accepted 17 June 2013; published online 21 June 2013)

Associate Editor Sean S. Kohles oversaw the review of this article.

Abstract—We used finite element (FE) method to investigate the effect of the drilling number and entry location of holes used in the multiple drilling technique on the stress and strain state in femur. Different three-dimensional FE models of a human hip joint with or without multiple drilling were fabricated using computed tomographic images obtained from the hip joint of a cadaver. The analysis technique was evaluated in a compression test using the cadaver specimen and FE analysis for the test using an FE model of the specimen. Von Mises stresses, principal stresses, and principal strains in the cancellous and cortical bone were calculated by using the different models, and changes in these values in relation to drilling number and entry hole locations were evaluated. Calculated peak values were much smaller than the yield strength, tensile strength, and yield strain of the cancellous and cortical bone for all cases of multiple drilling. Our results support that the multiple drilling technique for osteonecrosis of the femoral head is a stable operation technique.

Keywords—Core decompression, Multiple drilling, Early stage osteonecrosis, Finite element analysis, Femoral failure.

INTRODUCTION

Osteonecrosis of the femoral head is a recalcitrant disease. Although its pathogenesis is not completely understood, vascular occlusion and ischemia leading to osteocyte necrosis is a central concept. Vascular occlusion and ischemia can occur through three mechanisms: vascular interruption, extravascular compression, and thrombotic occlusion. These condi-

tions eventually lead to the death of osteocytes, subsequent collapse of the femoral head, and secondary hip joint osteoarthritis.¹

There are two surgical strategies for the treatment of osteonecrosis of the femoral head, depending on disease progression: femoral head preservation and femoral head replacement. Typically, operations on the femoral head in Ficat–Arlet stage I or II use femoral head preservation surgery,²⁸ such as core decompression,^{5,11,17,26} porous tantalum implants,²⁵ osteotomy,^{16,33} and bone grafting.³⁴ Operations on the femoral head in Ficat–Arlet stage III or IV use femoral head replacement,²⁸ such as total hip arthroplasty.^{18,21} Of the preservation surgeries, the core decompression technique, which can reduce intraosseous pressure and restore blood flow, is widely used due to its relative simplicity, short hospitalization period, and good clinical results.^{27,30}

Conventional core decompression has been conducted through a subtrochanteric approach with a single channel drilled by a large diameter (8–11 mm) trephine. However, this large channel can induce weakness of the femoral head and subtrochanteric region of the femur and thus lead to structural instability of the hip joint.⁵ As femoral fractures have been reported due to this instability, the multiple drilling technique for early stage osteonecrosis (Ficat–Arlet stage I, small lesions) has been proposed in order to reduce this risk. This technique uses multiple small diameter holes in contrast to the conventional technique.

Numerical studies for calculating principal stresses in femurs after core decompression by multiple small drilling holes showed that the multiple drilling

Address correspondence to Insu Jeon, School of Mechanical Systems Engineering, Chonnam National University, 300 Yongbong-dong, Buk-gu, Gwangju 500-757, Republic of Korea. Electronic mail: i_jeon@chonnam.ac.kr

technique provided a lower risk of bone fracture compared to conventional core decompression and core decompression with a tantalum osteonecrosis intervention implant.^{9,15} Clinical follow-up results have shown that the technique provides a successful treatment for osteonecrosis of the femoral head without serious complications.^{17,26} Nevertheless, also the multiple drilling technique presents risks of *femoral failure*, such as *yield* and *fracture*, due to stress concentration around the entry holes in the femoral subtrochanteric region. In order to decrease the risks from multiple drilling, minimization of the damage by drilling on the subtrochanteric region of the femur and drilling the overlapped entry hole has been recommended.^{5,26}

In this research, we used the finite element (FE) method to investigate the effects of drilling number and entry hole locations used in the multiple drilling technique on the von Mises stress, principal stress, and principal strain in the femur. Using the results, femoral failure after multiple drillings was evaluated. The suitability of FE models to evaluate human femur fractures has been investigated by Derikx *et al.*⁸ and Tanck *et al.*³¹ They compared FE analyses with experimental test results and concluded that the experimental load to failure for the intact and drilled femur could be predicted by the FE models. We also carried out a compression test using the intact hip joint and a 3D FE analysis of the compression test to evaluate our analysis technique. The aim of this study was to show that the multiple drilling technique for osteonecrosis of the femoral head is a stable operation technique.

MATERIALS AND METHODS

Three-Dimensional Reconstruction of a Hip Joint

We prepared a fresh cadaver without lesions or deformities of a 67-year-old male. It was a donated cadaver to the Catholic University of Korea, and we observed the guideline of Catholic Institute for Applied Anatomy for usage of donated cadavers. The femur of the cadaver had geometry (126.6° of the Caput–collum–diaphyseal angle and 13.7° of the femoral anteversion) and bone quality (1.060 g/cm³ of bone mineral density and a T score of -0.2). CT images were taken at intervals of 1 mm in the axial plane at a neutral anatomical orientation using a 128-channel volume CT scanner (Definition AS+; Siemens, Germany). We used a field of view of 250 × 250 mm, an optimal pixel size of 0.49 mm, and a resolution of 512 × 512 pixels as acquisition parameters for the CT images. We used the commercial software MIMICS (v10.1; Materialise, Belgium) with the CT images to reconstruct the sacroiliac joint

and hip joint including the sacrum, coxal bone, femur, sacroiliac cartilage, acetabular cartilage, and femoral head cartilage. The articular cartilages were manually reconstructed using the gaps between the sacrum and the coxal bone and between the coxal bone and the femoral head in the CT images because the detailed structure of soft tissue cannot be determined with X-ray CT system.

Geometric Modeling and Necrotic Region Definition

A geometric solid model using each reconstructed model of the intact hip joint was fabricated using the software Rapidform 2006 (Inus Technology Inc., Korea) (Fig. 1a). In order to reduce the difficulties for whole solid modeling, only half of the sacrum was modeled based on the symmetric structure of the lower extremity. The geometric model of the necrotic femur was developed through defining the necrotic region in the femoral head. This region was determined based on the angles in the mid-coronal and mid-sagittal images of the femur. Both angles were set at 100° corresponding to the extent of early stage small necrosis as classified by Koo and Kim¹³ (Fig. 1b).

Three geometric models of the necrotic femur after multiple drilling operations were fabricated through Boolean operations as virtual surgical operations (Fig. 1c).²⁶ An entry hole in the subtrochanteric region of the femur was defined as an overlapped hole of two drillings of 3.2 mm diameter in different directions toward the necrotic region. Therefore, models fabricated with 3, 5, and 7 entry holes in the subtrochanteric region contained 6, 10, and 14 drilling channels, respectively.

Two geometric models of short hole distance and changed entry hole position with 7 entry holes and 14 drilling channels were fabricated. In the short hole distance model, the distance between holes was decreased to half the hole radius. In the changed hole position model, all holes were assumed to be drilled in the subtrochanteric region close to the posterior region (Fig. 1d).

Finite Element Modeling and Material Properties

In the geometric solid models of the intact hip joint and the necrotic femurs with or without drillings, 3D FE meshes were generated using the commercial software PATRAN (v2008, MSC Software Corporation, USA) (Fig. 2). The hip capsular ligaments (iliofemoral, ischiofemoral, and pubofemoral ligaments) were attached to the 3D FE models as 1D truss elements based on the physiological cross-sectional area (PCSA).¹⁰ The muscles were attached to the models as 1D spring elements. A quadratic tetrahedral solid element

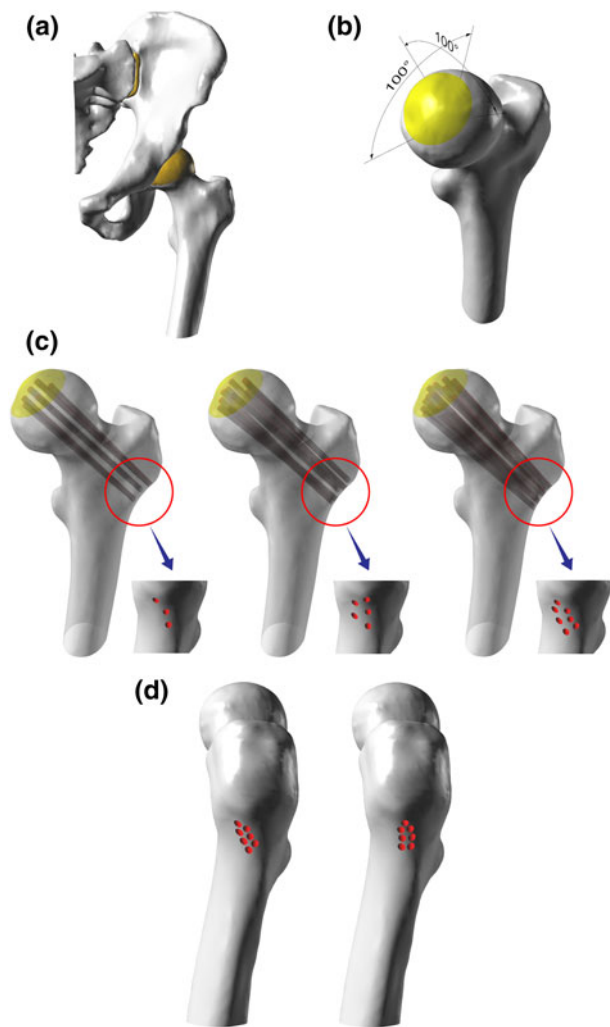


FIGURE 1. (a) A geometric solid model of the intact hip joint; (b) the determined necrotic region in the femoral head; (c) geometric models of the necrotic femur after multiple drilling operations; (d) the short hole distance model and changed entry hole position model.

with 10 nodes was used for all the bony structure models, and a quadratic tetrahedral hybrid continuum element with 10 nodes, which is suitable for hyperelastic material, was used for the sacroiliac, acetabular, and femoral head cartilage. For the entire FE model, fine FE meshes of 537,000 elements and 811,000 nodes were used, and very fine meshes were used around the drilling entry holes (Fig. 2). With these specifications we assumed that the calculated results would be insensitive to further refinement or to an increase in the number of elements.

The bony structures were assumed to be homogeneous, isotropic, and linear elastic.^{3,6} The articular cartilages were considered as homogeneous, incompressible, and hyperelastic in the neo-Hookean or Mooney–Rivlin models.^{14,23} In particular, the early stage necrotic region in the femoral head was assumed

to be a homogeneous, isotropic, linear elastic material. Its elastic modulus was determined by using the equation $E = 1904\rho^{1.64}$,³² where ρ is the average apparent density of the necrotic region defined as ρ (g/cm^3) = 0.0013 (HU) + 0.103.¹⁹ The Hounsfield units (HU) were obtained from CT images of the early stage osteonecrosis in the femoral head. All material properties used for the calculations are shown in Table 1.^{3,6,10,14,19,23,32}

Loads and Boundary Conditions

For loading conditions, we assumed the mid-stance phase (single leg support) of a patient corresponded to 30% of the gait cycle. An axial load of 570 N, which is 5/6 of 70 kg body weight,^{22,24} was applied to the sacrum through the center of the L5S1 disc and the facet of the sacral horn. These locations were selected in order to realistically apply body weight and suitable adduction moments to the hip joint models.³² In addition, the muscle contractile forces acting around the proximal femur were considered; these were decided from body weight.²⁹ For boundary conditions, the x-direction displacements of the nodes on the symmetric surfaces of the sacrum and coxal bones were constrained, and the nodes on the distal end of the femur were fixed to prevent translation and rotation (Fig. 2). The contact surface between the acetabular cartilage and the femoral head cartilage was defined with a friction coefficient of 0.01. FE analysis for each model was performed using the commercial software ABAQUS (v6.8.1, Dassault Systemes, France).

Evaluation of Finite Element Analysis Technique

Before FE analysis of the multiple drilling technique, we evaluated the analysis technique. A compression test was performed using the cadaver that was used to take the CT images. As a specimen for the compression test, the coxal bone and the femur with the acetabular cartilage and femoral head cartilage of the cadaver were preserved; all other soft tissues were removed. The upper part of the coxal bone and the distal part of the femur were embedded in epoxy resin and oriented in a neutral anatomical position. They were then mounted on the test jig of a universal testing machine (Instron 5567, Norwood, USA) (Fig. 3a). A super low-range (0.5–2.5 MPa) pressure sensitive film (LLW, Fuji, Japan) was used to measure contact pressures between the acetabular cartilage and the femoral head cartilage. To avoid artificial errors from film crinkle, the film was cut according to a rosette pattern based on the femoral head diameter and was used to wrap up the femoral cartilage (Fig. 3a). The

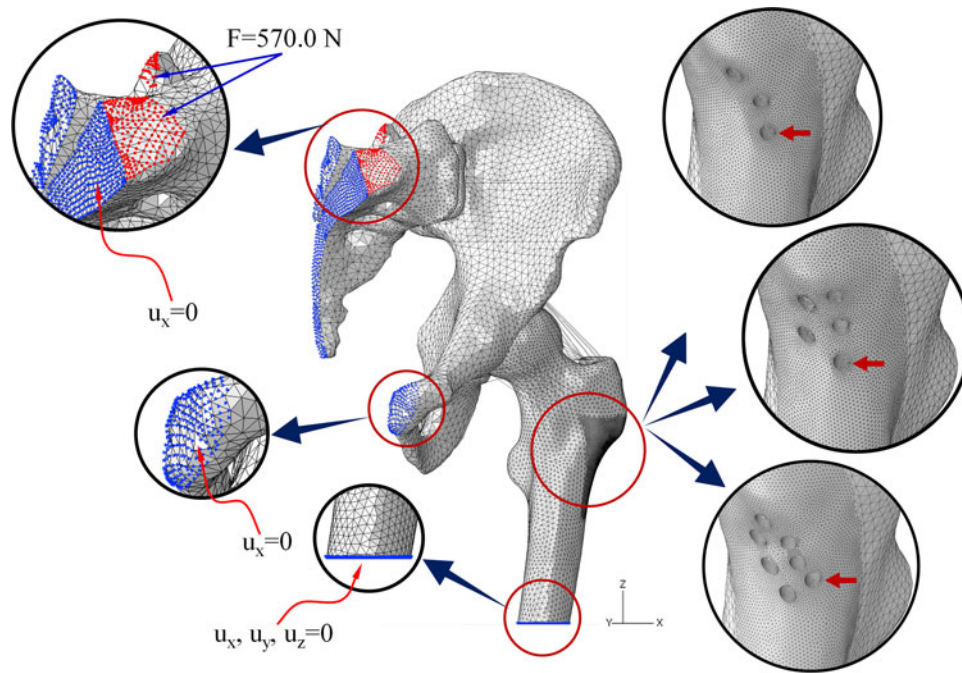


FIGURE 2. FE model of the hip joint with or without femoral drillings and its boundary conditions.

TABLE 1. Material properties used for the analysis.

Tissue	E-modulus (MPa)	Poisson's ratio	
Sacrum ⁶	17,000.0	0.30	
Coxal bone (cortical/cancellous) ⁶	17,000.0/70.0	0.30/0.20	
Femur (cortical/cancellous) ³	15,100.0/445.0	0.30/0.22	
Early necrotic femur ^{19,32}	332.9	0.3	
	E-modulus (MPa)	PCSA (mm ²)	Poisson's ratio
Iliofemoral ligament_Superior ¹⁰	113.3	120	0.40
Iliofemoral ligament_Inferior ¹⁰	242.2	92	0.40
Ischiofemoral ligament ¹⁰	99.5	81	0.40
Pubofemoral ligament ¹⁰	98.0	98	0.30
Articular cartilages ¹⁴	Mooney-Rivlin,		
(Sacrum and Acetabulum)	$C_{10} = 4.1$ MPa, $C_1 = 0.41$ MPa, $D_1 = 0$		
Femoral head cartilage ²³	Neo-Hookean, $G = 13.6$ MPa		

specimen was then vertically loaded up to 500 N through the coxal bone for 60 s.

This test process was simulated using FE models of the coxal bone and the femur with articular cartilages that were constructed using the CT images of the cadaver (Fig. 3b). Fine FE meshes of 137,593 elements and 203,734 nodes were used. All the same element types and material properties noted in the previous section were used for the FE models with the exception of the epoxy resin. We assumed that the epoxy resin was an elastic material with the elastic modulus $E = 2.5$ GPa and a Poisson's ratio $\nu = 0.35$. The same loading and boundary conditions of the compression test were applied for the FE analysis. We then

compared the measured contact pressures and the calculated values.

RESULTS

For the evaluation of the FE analysis technique, we compared the obtained peak contact pressure and the contact pressure distribution from the compression test and the FE analysis (Fig. 3c). The peak contact pressures were 2.45 MPa and 2.39 MPa from the compression test and FE analysis, respectively. The concentrated pressure regions obtained from both methods were located in the anterior part of the

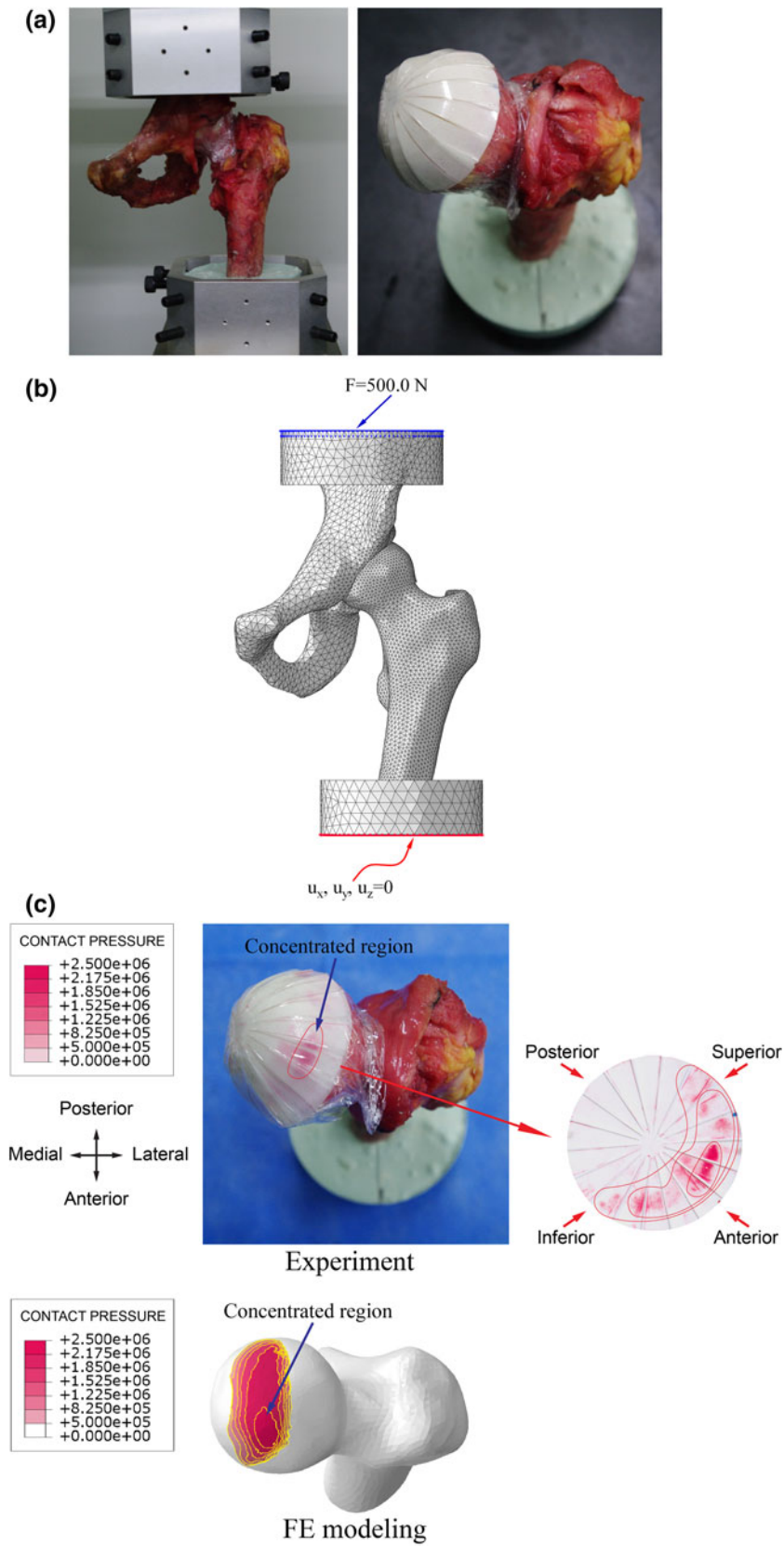


FIGURE 3. (a) The compression test setup and wrapped femoral head using the pressure sensitivity film; (b) its FE model and boundary conditions; (c) obtained contact pressure distributions.

femoral cartilage. The two methods showed similar patterns of contact pressure distribution in the femoral cartilage (Fig. 3c). This confirmed the applicability of our FE analysis process to analyze the effects of the multiple drilling technique.

To evaluate the effects of drilling numbers on femoral failure, the von Mises stress, principal stress, and principal strain of the femur were calculated and compared with the yield stress, tensile strength, and yield strain of the femur, respectively. Figure 4a shows the von Mises stress distributions of the intact femur model and the model with 14 drilled channels in the subtrochanteric region. The stress distribution of the subtrochanteric region close to the posterior region of the femur in the intact femur model was higher than that of the other region. In the 14 channel model, we found increased stress around the entry holes compared with the stress distribution in the intact femur model. The highest stress concentration was found around the entry hole at the subtrochanteric region close to the posterior region. In Fig. 4b, the principal strain distributions in the intact femur model and the 14 channel drilling model were compared. The 14 drilling model showed increased principal strain distributions, with the highest strain concentration found around the entry hole in the same region having the highest concentration of von Mises stress.

The peak values of the von Mises stress in the cancellous and cortical bone are plotted in Fig. 5a. No notable changes in peak values were found between the intact model and the necrotic femur model; these showed stresses of 0.39 and 0.40 MPa in the cancellous bone and 9.20 and 9.35 MPa in cortical bone, respectively. However, peak values in the drilling model changed in relation to the number of drillings. For 6, 10, and 14 drilling models, the values were 0.64, 0.65, and 0.71 MPa in the cancellous bone and 23.55, 23.13, and 31.17 MPa in the cortical bone, respectively. Our results indicated that all the values for the cancellous and cortical bones were less than the yield strength of 2.44 MPa for the cancellous bone²⁰ and 104 MPa for the cortical bone.²

Figure 5b shows the peak values of the principal stress in the cancellous and cortical bone. The peak value trend changed depending on the number of drillings and was similar to that of the von Mises stress. In the intact and necrotic femur models, we obtained approximately the same peak values for the cancellous bone (0.25 and 0.26 MPa, respectively) and cortical bone (9.30 and 9.54 MPa, respectively). For the 6, 10, and 14 drilling models, the values were 0.72, 0.74, and 0.86 MPa in the cancellous bone and 23.94, 23.24, and 31.57 MPa in the cortical bone, respectively. We also found that all the values were small compared with the tensile strengths of the cancellous

and cortical bone, which were 3.5 MPa⁷ and 122 MPa,¹² respectively.

The peak values of the principal strain in the cancellous and cortical bone are plotted in Fig. 5c. In the intact and necrotic femur models, the peak values were 669×10^{-6} and 678×10^{-6} in the cancellous bone and 600×10^{-6} and 610×10^{-6} in the cortical bone, respectively. Similar peak values of the principal strain in the cancellous and cortical bone were observed in both models. Peak values for the 6, 10, and 14 drilling models increased compared to those of the intact model to 1528 , 1526 , and 1766×10^{-6} in the cancellous bone and to 1570 , 1533 , and 2070×10^{-6} in the cortical bone. The obtained values showed that all the peak principal strain values of both the cancellous and cortical bone were less than the yield strain of 6100×10^{-6} of the cancellous bone²⁰ and 6800×10^{-6} of the cortical bone.⁴

The 6 drilling and 10 drilling models showed similar peak values for von Mises stress, principal stress, and principal strain in the cancellous and cortical bones, while the 14 drilling model showed increased peak values compared to 6 and 10 drilling models. These results were related to the locations of the entry holes in the subtrochanteric region because the location of the nearest entry holes to the posterior region for both the 6 drilling and 10 drilling models were approximately the same (arrows, Fig. 2). Similar peak values of all the parameters were found around the holes. However, one entry hole of the 14 drilling model was closer to the posterior region than the holes of the 6 and 10 drilling models. The higher peak values were found around the hole.

To evaluate the effects of entry hole location, two models of short hole distance and changed entry hole position with 7 entry holes and 14 drillings were used for calculation of the von Mises stresses in the femur (Fig. 4c). We found that the models did not show a broad region of concentrated stresses. The calculated peak values of von Mises stress in the two models were 33.13 and 27.03 MPa, respectively, and did not show a notable increase in peak values compared to those of the multiple drilling model prior to changing the entry hole location.

DISCUSSION

We used FE analyses with FE models of various multiple drillings to investigate the effects of drilling number and entry hole locations of the multiple drilling technique. The results showed that the peak values of von Mises stress, principal stress, and principal strain around the entry holes of the cortical bone and cancellous bone increased compared to those of the

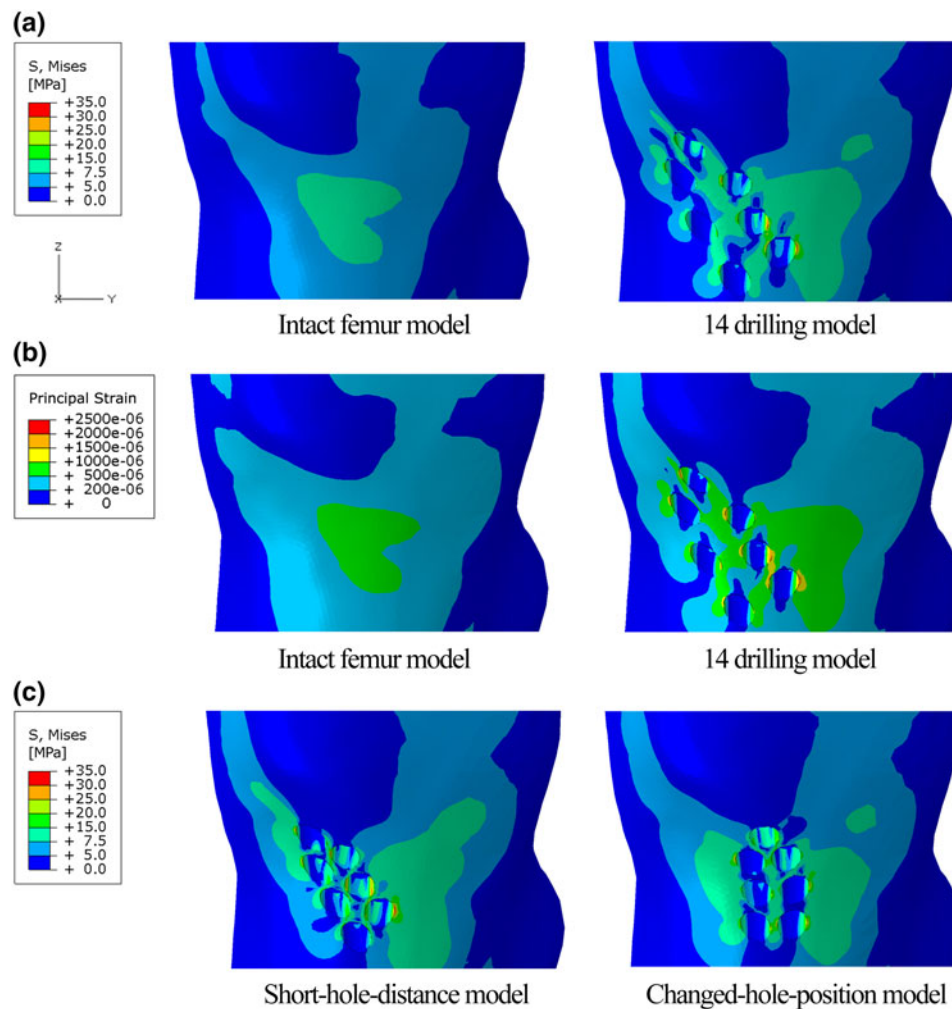


FIGURE 4. Representative distributions of (a) von Mises stress and (b) principal strain in the femur and (c) von Mises stress distributions in the cortical bone of the short hole distance model and the changed entry hole position model.

intact femur, depending on the number of drillings. However, in all cases of multiple drillings, these peak values were less than the yield strength, tensile strength, and yield strain of the cancellous and cortical bone. The effect of entry hole locations was also evaluated using a short hole distance model and a changed entry hole position model with 7 entry holes and 14 drillings. Both models showed that the changed location of entry holes did not increase peak values of von Mises stresses notably and did not broaden the region of concentrated stress compared to the multiple drilling model before the entry hole locations were changed.

An FE model of an entry hole with 5 drilling channels of 3.2 mm diameter in a femur was prepared by Floerkemeier *et al.*⁹ and Lutz *et al.*¹⁵ The model was used to calculate the maximum principal stresses around the entry hole under assumed loading cases, such as normal walking, walking down stairs, and accidental

stumbling. They found that multiple small drillings induce very low principal stresses in the femur compared with the tensile or compressive strength of the femur. Therefore, they concluded that the multiple small drilling technique is safe with respect to the risk of femur fracture. The clinical study of Mont *et al.*¹⁸ showed that no fractures were observed in 45 patients who were exposed to reduced weight bearing for 5–6 weeks.

Song *et al.*²⁶ used multiple drilling with an increased number of entry holes and drilling channels. They used Steinmann pins of 3.5 mm diameter to drill 2–8 entry holes with 4–22 drilling channels, depending on the lesion size, in the femoral head. Their clinical follow-up results showed that the multiple drilling operation was successful in 15 patients with small lesions, and these were without complications and reoperation after 5 years. These clinical results support the appropriateness of our numerical results because our results showed low calculated values of the von Mises stresses,

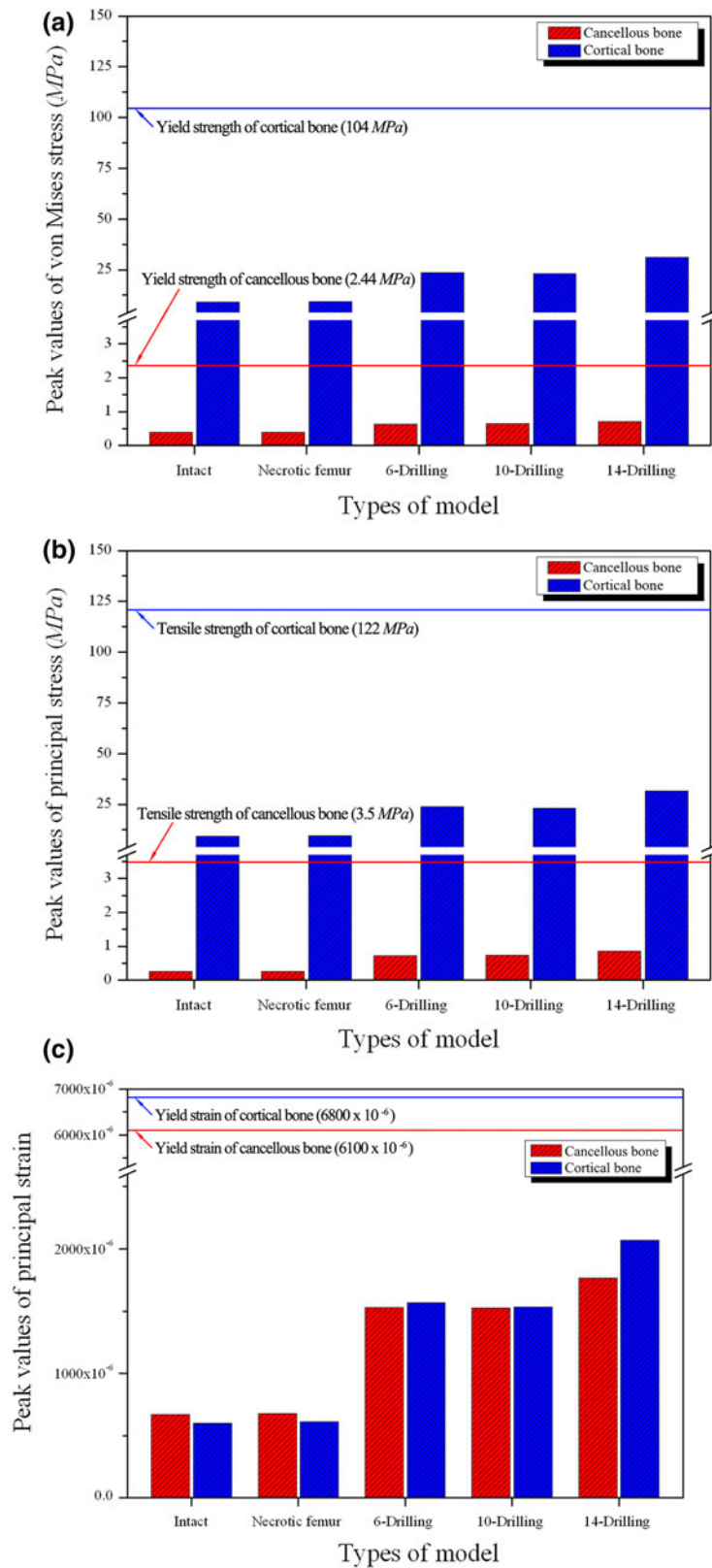


FIGURE 5. Peak values of (a) von Mises stress, (b) principal stress, and (c) principal strain in the cancellous and cortical bone according to the model type.

principal stresses, and principal strains in the femur compared to values for femoral failure.

This study has some limitations. First, only one loading state of normal walking (30% of the gait cycle) was considered as the applied load to the FE model of the hip joint. For more precise evaluation of the multiple drilling technique, FE analysis using the loading states of walking downstairs and accidental stumbling are needed. However, the resultant force of accidental stumbling, which is a severe loading state, is about two to three times that of a normal walk.¹⁵ Because of the large difference between the calculated peak values and femoral failure values (Figs. 5a–5c), we assumed that a similar result for the stability of the multiple drilling technique could be anticipated even though we applied the loading state of accidental stumbling.

Second, the material properties of each soft tissue assigned in this research were assumed to be homogeneous, isotropic, and linear elastic or hyperelastic in spite of more actual assumption for the material property, which was anisotropic and viscoelastic. In addition, effective elastic moduli were used for the cortical and cancellous bones except in the early stage necrotic region. To avoid the complexity of defining the material properties of muscles and ligaments, we adopted simple material behaviors, which have been documented by other researchers. The suitability of the assumed material properties of the cartilages, cortical bone, and cancellous bone was confirmed by our compression test.

Finally, we used only one cadaver specimen for the evaluation of our analysis technique. For the validation of our analysis technique, more cadaver tests and their FE analyses should be carried out and compared. However, our test results from the one test were in agreement with the results of the FE analysis.

In summary, we conclude that the multiple drilling technique for core decompression can be regarded as a considerably stable technique to prevent femoral failure. Based on our results, we suggest that commonly proposed long postoperative rehabilitation procedures, such as toe-touch weight bearing using crutches for 5–6 weeks, full weight bearing for 3 months, and high-impact loading (jogging and jumping) for 12 months, after the multiple drilling operation may be modified to a shorter rehabilitation period based on the age, bone mineral density, and weight of patients.

ACKNOWLEDGMENTS

This work was supported by the National Research Foundation of Korea (NRF) Grant funded by the Korea government (MEST) (No. 2012R1A2A2A01046128).

CONFLICT OF INTEREST

There are no conflicts of interest related to this manuscript.

REFERENCES

- ¹Aaron, R. K., and R. Gray. Osteonecrosis: etiology, natural history, pathophysiology and diagnosis. In: *The Adult Hip*, 2nd edition, edited by J. J. Callahan, A. G. Rosenberg, and H. E. Rubash. Philadelphia: Lippincott Williams & Wilkins, 2007, pp. 463–476.
- ²Bayraktar, H. H., E. F. Morgan, G. L. Niebur, G. E. Morris, E. K. Wong, and T. M. Keaveny. Comparison of the elastic and yield properties of human femoral trabecular and cortical bone tissue. *J. Biomech.* 37(1):27–35, 2004.
- ³Brown, T. D., M. E. Way, and A. B. Ferguson. Mechanical characteristics of bone in femoral capital aseptic necrosis. *Clin. Orthop. Relat. Res.* 156:240–247, 1981.
- ⁴Carter, D. R. Mechanical loading histories and cortical bone remodeling. *Calcif. Tissue Int.* 36:S19–S24, 1984.
- ⁵Colwell, C. W. The controversy of core decompression of the femoral head for osteonecrosis. *Arthritis Rheum.* 32(6):797–800, 1989.
- ⁶Dalstra, M., and R. Huiskes. Load transfer across the pelvic bone. *J. Biomech.* 28(6):715–724, 1995.
- ⁷Damien, C. J., and J. R. Parsons. Bone graft and bone graft substitutes: a review of current technology and applications. *J. Appl. Biomater.* 2(3):187–208, 1991.
- ⁸Derikx, L. C., J. B. van Aken, D. Janssen, A. Snyers, Y. M. van der Linden, N. Verdonshot, and E. Tanck. The assessment of the risk of fracture in femora with metastatic lesions: comparing case-specific finite element analyses with predictions by clinical experts. *J. Bone Joint Surg. Br.* 94(8):1135–1142, 2012.
- ⁹Floerkemeier, T., A. Lutz, U. Nackenhorst, F. Thorey, H. Waizy, H. Windhagen, and G. von Lewinski. Core decompression and osteonecrosis intervention rod in osteonecrosis of the femoral head: clinical outcome and finite element analysis. *Int. Orthop.* 35:1461–1466, 2011.
- ¹⁰Hewitt, J. D., R. R. Glisson, F. Guilak, and T. P. Vail. The mechanical properties of the human hip capsule ligaments. *J. Arthroplasty* 17(1):82–89, 2002.
- ¹¹Israelite, C., C. L. Nelson, C. F. Ziarani, J. A. Abboud, J. Landa, and M. E. Steinberg. Bilateral core decompression for osteonecrosis of the femoral head. *Clin. Orthop. Relat. Res.* 441:285–290, 2005.
- ¹²Ko, R. The tension test upon the compact substance of the long bones of human extremities. *J. Kyoto Pref. Med. Univ.* 53:503–525, 1953.
- ¹³Koo, K. H., and Kim, R. Quantifying the extent of osteonecrosis of the femoral head. A new method using MRI. *J. Bone Joint Surg. Br.* 77(6):875–880, 1995.
- ¹⁴Little, R. B., H. B. Wevers, D. Siu, and T. D. Cooke. A three-dimensional finite element analysis of the upper tibia. *J. Biomech. Eng.* 108(2):111–119, 1986.
- ¹⁵Lutz, A., U. Nackenhorst, G. von Lewinski, H. Windhagen, and T. Floerkemeier. Numerical studies on alternative therapies for femoral head necrosis: a finite element approach and clinical experience. *Biomech. Model. Mechanobiol.* 10:627–640, 2011.
- ¹⁶Matsusaki, H., M. Noguchi, T. Kawakami, and T. Tani. Use of vascularized pedicle iliac bone graft combined with

- transtrochanteric rotational osteotomy in the treatment of avascular necrosis of the femoral head. *Arch. Orthop. Trauma Surg.* 125(2):95–101, 2005.
- ¹⁷Mont, M. A., P. S. Ragland, and G. Etienne. Core decompression of the femoral head for osteonecrosis using percutaneous multiple small diameter drilling. *Clin. Orthop. Relat. Res.* 429:131–138, 2004.
- ¹⁸Mont, M. A., T. M. Seyler, J. F. Plate, R. E. Delanois, and J. Parvizi. Uncemented total hip arthroplasty in young adults with osteonecrosis of the femoral head: a comparative study. *J. Bone Joint Surg. Am.* 88:104–109, 2006.
- ¹⁹Moon, H. W., M. K. Lee, J. K. Kim, T. S. Lee, and K. W. Choi. The study of changes in compressive strength of trabecular bone with PMMA injection in vertebroplasty. *J. Biomed. Eng. Res.* 24(4):369–373, 2003.
- ²⁰Morgan, E. F., and T. M. Keaveny. Dependence of yield strain of human trabecular bone on anatomic site. *J. Biomech.* 34(5):569–577, 2001.
- ²¹Nich, C., J. P. Courpied, M. Kerboull, M. Postel, and M. Hamadouche. Charnley-Kerboull total hip arthroplasty for osteonecrosis of the femoral head a minimal 10-year follow-up study. *J. Arthroplasty* 21(4):533–540, 2006.
- ²²Nordin, M., and V. H. Frankel. Biomechanics of the foot and ankle. In: *Basic Biomechanics of the Musculoskeletal System* 3rd, edited by M. Nordin, and V. H. Frankel. Philadelphia, PA: Lippincott Williams & Wilkins, 2001, pp. 202–221.
- ²³Park, S., C. T. Hung, and G. A. Ateshian. Mechanical response of bovine articular cartilage under dynamic unconfined compression loading at physiological stress levels. *Osteoarthr. Cartil.* 12(1):65–73, 2004.
- ²⁴Perry, J. *Gait analysis: Normal and Pathological function*. Thorofare, NJ: Slack Incorporated, 1992.
- ²⁵Shuler, M. S., M. D. Rooks, and J. R. Roberson. Porous tantalum implant in early osteonecrosis of the hip: preliminary report on operative, survival, and outcomes results. *J. Arthroplasty* 22(1):26–31, 2007.
- ²⁶Song, W. S., J. J. Yoo, Y. M. Kim, and H. J. Kim. Results of multiple drilling compared with those of conventional methods of core decompression. *Clin. Orthop. Relat. Res.* 454:139–146, 2007.
- ²⁷Soohoo, N. F., S. Vyas, J. Manunga, H. Sharifi, G. Kominski, and J. R. Lieberman. Cost-effectiveness analysis of core decompression. *J. Arthroplasty* 21(5):670–681, 2006.
- ²⁸Steinberg, M. E. Management of avascular necrosis of the femoral head—an overview. *Instr. Course Lect.* 37:41–50, 1988.
- ²⁹Stolk, J., N. Verdonschot, and R. Huiskes. Hip-joint and abductor-muscle forces adequately represent *in vivo* loading of a cemented total hip reconstruction. *J. Biomech.* 34(7):917–926, 2001.
- ³⁰Stulberg, B. N., A. W. Davis, T. W. Bauer, M. Levine, and K. Easley. Osteonecrosis of the femoral head: a prospective randomized treatment protocol. *Clin. Orthop. Relat. Res.* 268:140–151, 1991.
- ³¹Tanck, E., J. B. van Aken, Y. M. van der Linden, H. W. Schreuder, M. Binkowski, H. Huizenga, and N. Verdonschot. Pathological fracture prediction in patients with metastatic lesions can be improved with quantitative computed tomography based computer models. *Bone* 45(4):777–783, 2009.
- ³²Wirtz, D. C., N. Schiffers, T. Pandorf, K. Radermacher, D. Weichert, and R. Forst. Critical evaluation of known bone material properties to realize anisotropic FE-simulation of the proximal femur. *J. Biomech.* 33(10):1325–1330, 2000.
- ³³Yoon, T. R., A. A. Abbas, C. I. Hur, S. G. Cho, and J. H. Lee. Modified transtrochanteric rotational osteotomy for femoral head osteonecrosis. *Clin. Orthop. Relat. Res.* 466(5):1110–1116, 2008.
- ³⁴Zhao, D., D. Xu, W. Wang, and X. Cui. Iliac graft vascularization for femoral head osteonecrosis. *Clin. Orthop. Relat. Res.* 442:171–179, 2006.